Journal of Membrane Science 466 (2014) 302–312

Contents lists available at ScienceDirect

Journal of Membrane Science

journal homepage: www.elsevier.com/locate/memsci

The effect of Tween-20 additive on the morphology and performance of PVDF membranes

Hsu-Hsien Chang [a], Sheng-Chang Chen [a], Dar-Jong Lin [a,b], Liao-Ping Cheng [a,b,*]

[a] Department of Chemical and Materials Engineering, Tamkang University, New Taipei City 25137, Taiwan
[b] Energy and Opto-Electronic Materials Research Center, Tamkang University, New Taipei City 25137, Taiwan

ARTICLE INFO

Article history:
Received 25 February 2014
Received in revised form
5 May 2014
Accepted 7 May 2014
Available online 13 May 2014

Keywords:
PVDF membrane
Surfactant
Macrovoid
Immersion precipitation
Ultra-filtration

ABSTRACT

The effects of additive, Tween-20, on the morphology and ultra-filtration performance of the PVDF membranes formed by isothermal immersion precipitation from the Tween-20/water/TEP/PVDF system were investigated. High resolution FESEM imaging indicates that the membranes' bulk constituted of interlinked crystalline particles, whose shapes change from more sheaf-like to more stick-like as larger amounts of Tween-20 were initially added into the dope. Introduction of Tween-20 caused formation of nano-pores on the top surfaces of the membranes and micron-sized columnar voids underneath the top skin layer. Some small amounts of Tween-20 may reside in the formed membrane if the nascent membrane has not been carefully washed. Presence of Tween-20 in the membrane was analyzed by water contact angle measurements, Fourier Transform Infrared-Attenuated total reflection spectroscopy (FTIR-ATR), Nuclear Magnetic Resonance (NMR), and X-ray Photoelectron Spectroscopy (XPS). Furthermore, water flux and blue dextran filtration experiments were carried out to illustrate the potential applications of the membranes in fine separation processes.

1. Introduction

Poly(vinylidene fluoride) (PVDF) is a hydrophobic polymer widely used to produce porous membranes for various industrial applications, thanks to its superior mechanical strength, thermal stability, and chemical resistance [1]. PVDF membranes are commonly prepared by the immersion–precipitation method, in which a polymer solution (termed dope) in the form of flat sheet, hollow fiber, or sphere is immersed in a non-solvent coagulant to invoke precipitation of the polymer. The nascent polymeric precipitate is subsequently washed and then dried to yield a porous membrane. It is generally found that strength of the coagulant (e.g., harsh or soft) and state of the dope (e.g., degree of supersaturation with respect to crystallization) are the key factors that govern porous structure outcomes [2,3].

Water is a typical *harsh* non-solvent that is frequently employed to prepare porous membranes. When a casting dope is immersed in it, precipitation occurs very rapidly (termed instantaneous demixing in the literature) to give the so-called asymmetric structure, consisting of a dense skin and a porous supporting bulk. The skin layer is known to derive from sharp polymer enrichment at the membrane–bath interface, whereas the porous bulk from liquid–liquid demixing [4]. Presence of a dense skin renders the membrane unsuited to sieving-based separation processes, e.g., micro- or ultra-filtration process, for which high permeation fluxes are demanded. Several methods have been adopted to trim down the possibility of skin layer formation, such as using a soft bath [2,3], changing the precipitation temperature [4], inducing nucleation in the casting dope [2], adding pore formers etc. [6–12]. Among them, using pore former is an effective approach not only to eliminate the dense skin but also to increase the porosity. Pore formers can be divided into three types: (1) inorganic salts, such as sodium chloride and lithium perchlorate [6], (2) oligomeric/macromolecular species, such as PVP [7] and PEG [8], pluronic copolymer [10], and (3) surfactants, such as sodium dodecyl sulfate (SDS) [11,12], TritonX-100 [11,13], Span-80 [14] etc. Because surfactant is amphiphilic, it could dissolve rapidly into the dope solution, and upon immersion it would out-flow into the coagulant bath quickly. Such mass transfer event results in break-opening of the top gel layer and introduction of pores on the top surface; henceforth, the formed membranes are useful for ultra- and nano-filtration processes. However, it is often noted that some surfactants may reside in the membrane, which in turn may affect the separation performance [10,12,13]. Therefore, it is useful to determine the quantity of

* Corresponding author at: Department of Chemical and Materials Engineering, Tamkang University, New Taipei City 25137, Taiwan. Tel.: +886 2 26215656x2725/2614; fax: +886 2 26209887.
E-mail address: lpcheng@mail.tku.edu.tw (L.-P. Cheng).

http://dx.doi.org/10.1016/j.memsci.2014.05.011
0376-7388/

surfactant left in the formed membrane. Such work, however, has not been seen in the membrane literature.

Zhao et al. added amphiphilic polymers in the casting dopes to fabricate PVDF membranes with porous top surface. Utilizing X-ray photoelectron spectroscopic analysis (XPS), they were able to identify additive residues in the formed membranes [15]. Amirilargani et al. used Tween-80 to modify the structure of poly(ether sulfone) membranes, and found that cellular pores and finger-like macrovoids amplified with increasing Tween-80 content in the dope [16]. Riyasudheen et al. prepared poly(ethylene-co-vinyl alcohol)/poly(vinyl pyrolidone) (EVAL/PVP) membranes by using the NIPS process. At low dosage of PVP, the formed membranes exhibited increased water permeation fluxes as a result of extensive macrovoids formation, while at high dosages, thick skin layer formed and the fluxes decreased [17].

Previously, we have prepared PVDF membranes by immersion–precipitation from the H_2O/TEP/PVDF system, and have investigated the influence of bath strength (i.e., concentration of TEP in the bath) on the membrane's porous structure [3]. Quite interestingly, it was found that all the membranes exhibited a bi-continuous cross-section packed by interlocked crystalline particles, irrespective of whether the bath being soft or harsh. No evidence of cellular pore formation was detected even precipitating the dope in the '*harsh*' water bath. The top surface, however, was dense and non-porous in most immersion cases, and only when the bath contained as high as ~70% TEP, would the dense skin be totally open-up, having a structure resembling the cross sectional region. Coagulation bath with such high solvent content is undesirable, as it is expensive, harmful, environmental unfriendly, and hard to maintain/dispose. Thus, in this research, a casting formulation is sought, whereby skinless bi-continuous membranes could be produced simply from water bath.

This was realized by incorporating the surfactant, Tween-20, as an additive to the casting dope. Given the fact that Tween-20 was prone to leave the casting solution during the course of immersion–precipitation, a robust and continuous top gel layer would not be formed. Moreover, as a metastable dope that is supersaturated with respect to crystallization was employed; formation of macrovoids was prohibited, as opposed to most other membrane systems incorporating a surfactant, for which large voids were prevalent [10–12,16,18]. The formed membranes were characterized by various techniques, e.g., FESEM for the morphology, FTIR, XPS and NMR for residual Tween-20 identification, XRD and DSC for the crystallinity, blue dextran ultra-filtration for the rejection capability etc. Based on the above results and documented theories, a preliminary porous structure formation mechanism was then proposed.

2. Experimental

2.1. Materials

Poly(vinylidene fluoride) (PVDF, Kynar740 from Elf Ato Chem, Mn=245,000 g/mol, d=1.78 g/cm^3) was obtained in pellet form. Triethyl phosphate, (TEP, Acros, d=1.07 g/cm^3) was used as the solvent for PVDF. Polysorbate-20 (Tween-20, J.T. Baker, d=1.11 g/cm^3) was used as an additive to the dope. Distilled/de-ionized water was used as the coagulant. Dimethyl sulfoxide-d_6 (DMSO-d_6, containing 0.1% TMS, Acros) was used as the d-solvent for NMR analyses of the formed membranes. Blue dextran (Mw=2,000,000 g/mol, Sigma Aldrich) was used as the solute for filtration experiments. All materials were used as received.

2.2. Membrane preparation

Flat-sheet type PVDF membranes were prepared by the isothermal immersion–precipitation method at room temperature.

Table 1
Preparation conditions and properties of PVDF membranes.

Code[a]	Dope composition (%)			Thickness (μm)	Bulk porosity (%)	Formation time[b] (s)	Tensile strength (N/mm^2)
	PVDF	TEP	Tween-20				
MA	18	82	0	82 ± 1	67.7 ± 0.3	22 ± 3	6.9 ± 0.6
MB	18	81	1	94 ± 1	73.4 ± 0.3	17 ± 2	3.6 ± 0.3
MC	18	79	3	109 ± 1	76.2 ± 0.2	13 ± 1	3.4 ± 0.1
MD	18	77	5	116 ± 4	80.2 ± 1.7	11 ± 1	2.3 ± 0.2
ME	18	74.5	7.5	128 ± 2	80.9 ± 1.8	8 ± 1	2.3 ± 0.3
MF	18	72	10	147 ± 2	81.1 ± 1.3	5 ± 1	2.2 ± 0.2

[a] Bath: pure water at 23 °C.
[b] Deviation based on the Excel STDEV method for 5 experimental runs.

Appropriate amounts of PVDF, TEP, and Tween-20 (Table 1) were mixed in a glass bottle sealed with a Teflon-lined cap. The mixture was blended at 80 °C on a roller until it became a homogeneous polymer solution (called dope, hereinafter). The dope was cooled to room temperature (23 ± 1 °C, taking ca. 20 min), uniformly spread on a glass plate using an applicator with a clearance of 250 μm, and then immersed in a water bath. After precipitation was completed (typically in a few minutes), the nascent membrane was detached from the glass plate, and then washed repeatedly in water and ethanol to remove TEP and residual Tween-20. Finally, the formed membrane was held in light press between two sheets of filter papers and dried at 50 °C in a convective oven. The immersion conditions for various membranes are summarized in Table 1.

2.3. Membrane characterization

(1) Morphologies of the membranes were observed using a field emission scanning electron microscope (FESEM, Leo1530, Carl Zeiss, Germany). Membrane samples were vacuum-dried and then an appropriate size of the top, bottom, or cross sectional area was attached to a sample holder using conductive cooper tapes. The cross section was obtained by fracturing the membrane in liquid nitrogen. Silver paste was applied at the edges of the sample to enhance electronic conductivity. Then, the sample was sputtered with a layer of Pt–Pd alloy (~2 nm) and observed under a low acceleration voltage (2.5 kV) by means of an in-lens detector. The pore size and porosity in the SEM micrographs were measured using the software, Image J, 1.44p.

(2) The porosities of the membranes were determined by the following equation:

$$\text{Porosity}\ (\%) = \frac{(V_m - V_p)}{V_m} 100\%$$

where V_m is the bulk volume of the membrane and V_p is the volume of polymer in the membrane. V_m was obtained by multiplying the membrane area by its thickness, as was measured by a thickness gauge. V_p is equal to W_m/ρ_p, where W_m is the weight of the membrane and ρ_p is the density of the polymer (ρ_p=1.78 g/cm^3 for PVDF).

(3) The tensile strength at the breaking point for various membranes was determined according to ASTM (D638 Type V) using a universal testing machine (AGS-J SHIMADZU, Japan) at the crosshead speed of 1 mm/min and maximum load of 500 N. At least 5 samples were examined for each membrane, and the average value was reported with deviation.

(4) The contact angles of the membranes were measured by a contact angle/surface tension analyzer (FTA 125, First Ten Angstrons, USA) at room temperature. A drop of water (2 μl)

was deposited on the surface of the membrane. Image of the water drop was taken and the contact angle was measured from shape analysis. To ensure reliable data being obtained, 5 measurements at different locations of the membrane surface were taken and the average value was reported together with the deviation.

(5) The infrared absorption spectra of the PVDF membranes were obtained by a Fourier Transform Infrared-Attenuated Total Reflection spectrometer (FTIR-ATR, NicoletiS10, Thermo, USA) at a resolution of 4 cm^{-1} with 32 scans over the wavenumber range of 400–4000 cm^{-1}.

(6) Nuclear magnetic resonance (^{1}H NMR) spectroscopy was employed to determine the amount of residual Tween-20 in the PVDF membrane. The spectra were obtained on a NMR spectrometer (Avance AVII 600, Bruker, Germany) operated at 600 MHz. Deuterated DMSO-d_6 was used as the solvent for the membrane samples. The amount of Tween-20 resided in the membrane (R_{NMR}) was calculated by the following equation [19]:

$$R_{NMR} = \frac{A_S(M_S/n_S)}{(A_S(M_S/n_S)) + (A_P(M_P/n_P))} 100\% \quad (1)$$

where A_s denotes the area of the peak assigned to the ethylene oxide groups of Tween-20 (δ=3.5 ppm), while A_p to the repeat unit of PVDF (δ=2.9 ppm). M_s and M_p are, respectively, the molecular weights of Tween-20 and repeat unit of PVDF (M_s=1226 g mol^{-1}, M_p=64 g mol^{-1}). n_s and n_p are the total number of hydrogen atoms on the ethylene oxide group and on the repeat unit of PVDF, respectively. n_s is equal to 80 whereas n_p is equal to 2.

The efficiency of Tween-20 removal can be calculated by the following equation:

$$\text{Extraction } (\%) = \left(1 - \frac{R_{NMR}/(1-R_{NMR})}{D_{T20}/D_{PVDF}}\right) 100\%$$

where D_{T20} and D_{PVDF} refer to the weight percentages of Tween-20 and PVDF in the casting dope, respectively. For example, for preparing the membrane "MD", D_{T20}=5% and D_{PVDF}=18%, and from the NMR analysis, R_{NMR}=0.35%. Therefore, the removal efficiency is 98.7%.

(7) The compositions of Tween-20 near the top surface of the membranes were analyzed by the X-ray photoelectron spectroscope (XPS, VG ESCA Scientific Theta Probe, England). Al K_α radiation (1486.6 eV) was used as the X-ray source with an X-ray spot size of 400 μm. The Tween-20 content (R_{XPS}) in the vicinity of the membrane surface can be calculated by the following equation:

$$R_{XPS}\ (\%) = \frac{(P_o - P_o')(M_S/N_S)}{((P_o - P_o')(M_S/N_S)) + (P_F(M_P/N_P))} 100\% \quad (2)$$

where P_o and P_o' represent the detected atomic percentages of oxygen on the membrane surface and the background respectively (background oxygen=1.99%, tested using membrane prepared from dope free of Tween-20). P_F is the percentage of fluorine atoms in the membrane. M_s and M_p are the molecular weights of Tween-20 and repeat unit of PVDF respectively. N_s and N_p are the number of oxygen atoms in a Tween-20 molecule (26) and the fluorine atoms in each repeat unit of PVDF (2), respectively.

(8) Pure water fluxes of the prepared membranes were measured by a dead-end cell (effective area=11.34 cm^2) with trans-membrane pressures of 1–4 kg/cm^2 corresponding to micro- and ultra-filtration operations. The membrane was pre-wetted in 2-propanol first, and then its water fluxes were measured at room temperature. For each measurement, water was collected after stable flux being attained; the collection time was ca. 1–30 min, depending upon the efflux rate.

(9) Solute rejections of the membranes were determined using a 3.8 cm diameter dead-end stirred cell at a stirring speed of 300 rpm. The solute employed in the present work was blue dextran with an average molecular weight (g/mole) of 2000 kDa (Sigma). The feed solution was prepared by dissolving blue dextran in distilled–deionized water at the concentration of 0.1 wt%. The operation temperature was 25 °C and the trans-membrane pressure was 2 kg/cm^2 for all measurements. After the permeation flux reached a stable value, samples of filtrate were collected for subsequent UV colorimetry (UV–visible Spectroscopy, Heλiosβ, Unicam, UK). The concentrations of the solute in the feed (C_b) and the filtrate (C_f) were used to calculate the rejection coefficient (R) based on the following equation:

$$R = \left(1 - \frac{C_f}{C_b}\right) 100\%$$

3. Results and discussions

3.1. Morphology, porosity, and mechanical property of the membranes

PVDF tends strongly to crystallize when the casting dope is brought into the phase separation boundary in the immersion–precipitation process. The formed membranes often exhibit particulate morphologies composed of stick-, sheaf-, or sphere-like crystallites that represent different stages of spherulitic growth, depending on the dope and bath conditions [3,20]. In Fig. 1, the cross-sectional SEM images of the membranes prepared by immersing casting dopes containing different amounts of Tween-20 in a water bath are demonstrated. For the membrane "MA", the crystalline particles appear spherical-shaped with an identifiable size of ~2–3 μm. Upon gradual increase of Tween-20 content in the dope, the particle size decreases and the particle shape shifts towards sheaf- or stick-like form. For instance, as revealed clearly in the high magnification images (insets), the crystallites in the membrane "MC" still bear some resemblance of a sphere (<2 μm), and yet those in the membrane "MF" become essentially stick-like (<1 μm). The nano-scale fine structure of the membrane "MF" is shown in Fig. 1(d). It is interesting to see that the stick-like entities are actually stacks of twisted/curled lamellae with thickness measured to be ~15 nm. Structural details of various PVDF membranes can be found in our previous publications [3]. The above morphological evidences, particularly the size and shape of crystallites, suggest that Tween-20 has played the role of enhancing polymeric crystal nucleation in the casting dope, in addition to acting as a pore former. This is verified further by comparing the measured crystallization times (the time required to form crystalline gel) for the dopes, which are 39, 35, 13, 8, 1.3, and 0.33 h, correspondingly, for the dopes "A–F". It should be noted that these dopes are in the metastable state with respect to crystallization with compositions within the crystallization boundary [3].

In addition to crystal structures in the cross section, Fig. 1 also indicates the presence of parallel columnar voids just underneath the top surfaces of the membranes "MB–MF" that were prepared from dopes containing different amounts of Tween-20. Although these voids looked as if they were "finger-like macrovoids" commonly seen in PVDF membranes precipitated from harsh baths, they are in fact much smaller, with length of only ~1/10 of the membrane thickness and width of ~1 μm. The reason why MA does not exhibit columnar voids and why columnar voids of "MB–MF" are comparatively short can briefly be explained as follows. When the casting solution of dope "A" contacts the harsh nonsolvent (water) upon immersion, a robust gel layer will soon

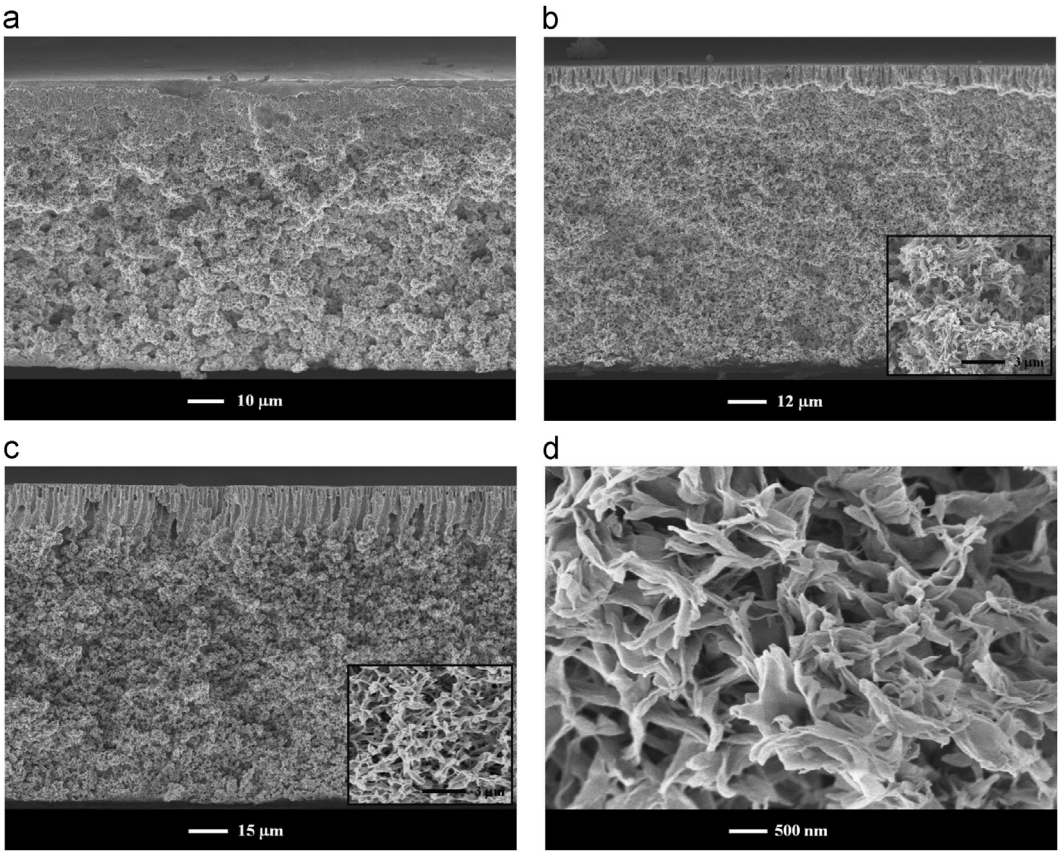

Fig. 1. SEM micrographs of cross sections of PVDF membranes after the addition of Tween-20 in the casting dope: (a) 0%, MA; (b) 3%, MC; (c) 10%, MF; and (d) high magnification image of MF.

be generated at the membrane–bath interfacial region due to a rapid boost of polymer concentration hereby [4]. This layer undoubtedly hampers further influx of water (also out-flux of solvent) molecules that are required to induce liquid–liquid demixing. Meanwhile, because dope "A" is in the incipient meta-stable state, it crystallizes easily upon slight concentration fluctuation to set in the particulate structure shown in Fig. 1. As a result, membrane "MA" consists of a dense skin and a uniform bulk without evidence of cellular pores. In contrast, when dopes "B–M" are immersed in water, Tween-20 tends strongly to leave the casting solution along with the out-diffusing TEP (as is validated by the NMR analysis shown later). This activity forbids the formation of a *continuous* top gel layer, and hence, water molecules can enter the casting film easily through the openings to induce liquid–liquid demixing. The phase-separated liquid domains (i.e., polymer-lean phase, composed essentially of solvent and nonsolvent) later-on develop into the observed columnar voids driven by osmotic forces [5,21]. However, during growth of the liquid domains, crystallization also takes place, and the growing crystallites obstruct the downward advancement of liquid domains such that the columnar voids are short and limited to the top region of the membrane.

The phase demixing rate is a factor useful for judging whether or not finger-like macrovoids will form in the immersion–precipitation process – generally, instantaneous demixing favors macrovoids formation whereas delayed demixing disfavors it [4]. Because Tween-20 and water are highly solvable mutually, they would exchange instantly upon their contact at immersion. Such rapid mass transfer events certainly promote fast phase demixing, which is confirmed by the decreased precipitation times for various immersion cases. As shown in Table 1, it takes about 22 s to visually observe cloudiness on casting film of dope 'A', yet it drops to 5 s after 10% Tween-20 is added (i.e., the membrane "MF"). Although the above visual precipitation times may deviate (most likely longer) from what were obtained by standard light transmission experiment, the values are over a reasonable range, agreeing with those reported in the literature. The fact that surfactants are able to speed-up phase demixing and lead to macrovoids structure has been reported by many authors [10–12,16,22]. For example, Loh et al. used Pluronic F127 as a pore former to prepare membranes from the H_2O/NMP/PVDF system, and found that finger-like macrovoids were more prominent as casting dopes that contained higher amounts of surfactant [22]. In fact, with addition of merely 1% of surfactant, macrovoids would already be observed to occupy most of the membrane cross section. Similar results can be found for preparation of polyethylsulfone membranes from dopes containing different types of surfactants, such as TritonX-100, SDS, CTAB, etc. [10,11,16]. In all these cases, very large macrovoids are present; the length of macrovoids could be as long as 100–150 μm, occupying almost half or even full of the membrane cross section. Large macrovoids are undesirable since they can significantly lower down the mechanical strength of a membrane. For the present Tween-20/H_2O/TEP/PVDF system, it is of special interest to find that finger-like columnar voids formation depends weakly on the surfactant dosage of the dope; even after adding 10% Tween-20 in the casting dope, the columnar voids are still very small with a length of ~22 μm, consisting ~1/7 of the membrane cross section. As mentioned earlier, rapid crystallization in the metastable dope, which inhibits downward growth of the liquid domains is thought to be the main cause.

Another effect of Tween-20 that merits notice (although not frequently addressed in the literature) concerns the generation of nano-pores on the top surface of the membrane, which is illustrated in Fig. 2 in terms of high magnification SEM images.

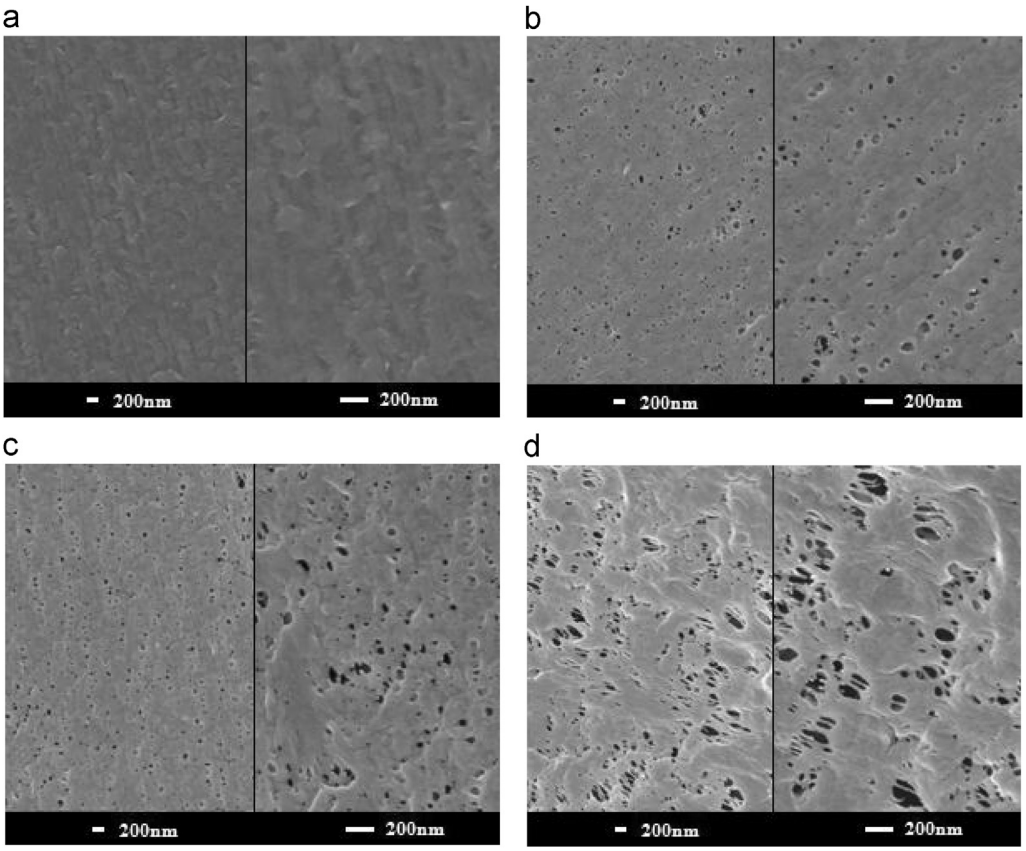

Fig. 2. SEM micrographs of the top surfaces of PVDF membranes after the addition of Tween-20 in the dope: (a) MA; (b) MC; (c) MD; and (d) MF.

The membrane "MA" has a dense skin layer, free of pores at a resolvable length-scale of ~10 nm. After adding just 1% of Tween-20 in the dope, nano-pores start to appear on the top surface. Increasing Tween-20 dosage increases the pore size and porosity (fraction of pore area on the surface) of the surface, of which the values determined based on image analysis are listed in Table 2. For example, the pore size and porosity are 26 nm and 1.9% for the membrane "MB", and become 43 nm and 15% for the membrane "MF". Such results clearly demonstrate the capability of Tween-20 to create nano-pores by breaking the top gel layer as they gush into the coagulation bath upon immersion. The uncommon morphological features – nano-porous selective layer plus bi-continuous cross section – enable the membranes applicable to the micro- or ultra-filtration process, as will be discussed later in the section regarding water flux and solute rejection. The surface nano-pores observed in Fig. 2 actually penetrate through the skin layer and connect with the pores in the cross section, as is evident from the high resolution images shown in Fig. 3. From these images, thicknesses of the skin layers for various membranes can be estimated, and the results are summarized in Table 2. Apparently, incorporating Tween-20 has effectively reduced the thickness of the skin layer from 64 nm (membrane "MA") to 14 nm (membrane "MF"), which may be related to the liquid–liquid demixing events (cellular pores can be seen in addition to finger-like voids) following the initial out-flux activities of Tween-20. However, the real causes are yet to be delineated at this stage.

It is found that the bottom surfaces of the membranes are less affected by Tween-20, as the surfactant would leave this region and migrate upwards (through the continuous liquid channels within the polymer-rich phase) during the precipitation process. For illustration, Fig. 4 shows high resolution images of the bottom surfaces of the membranes "MA" and "MF". Here, the spherulites

Table 2
Surface properties of the prepared membranes.

Code	Skin layer thickness (nm)	Surface pore size[a] (nm)	Surface porosity[a] (%)	Finger length (μm)	Top surface contact angle (deg)	Bottom surface contact angle (deg)
MA	64	–	–	–	82 ± 1	108 ± 2
MB	58	26	1.9	5	83 ± 2	118 ± 5
MC	23	33	3.9	6	82 ± 3	118 ± 3
MD	17	31	5.5	10	83 ± 3	114 ± 1
ME	14	32	7.5	12	86 ± 3	116 ± 2
MF	14	43	15.0	22	86 ± 2	121 ± 2

[a] Analyzed by the software (Image J 1.44p), the error value is standard deviation.

for "MA" are sheaf- or sphere-like, while those for "MF" are stick-like; they both resemble the crystallites in their respective cross sections, yet with a flattened feature arising from growth against the glass substrates [2,3,5].

3.2. Residual amount of Tween-20 in the membrane

As pointed out in the literature, the pore-forming surfactants added to the dope may eventually reside in the formed membrane [6,10,12,13]. In the present study, FTIR, NMR, and XPS were employed to see whether Tween-20 has been removed totally or not after the washing steps. In Fig. 5, the FTIR spectra of various prepared membranes are shown. The fingerprints of PVDF are located over the range of 650–1500 cm^{-1}; the strong absorptions at 766, 874, 976, and 1181 cm^{-1} are characteristics of the α-type crystals, whereas the weak shoulder-like band at 1279 cm^{-1} indicates the presence of a small amount of β-type crystals in

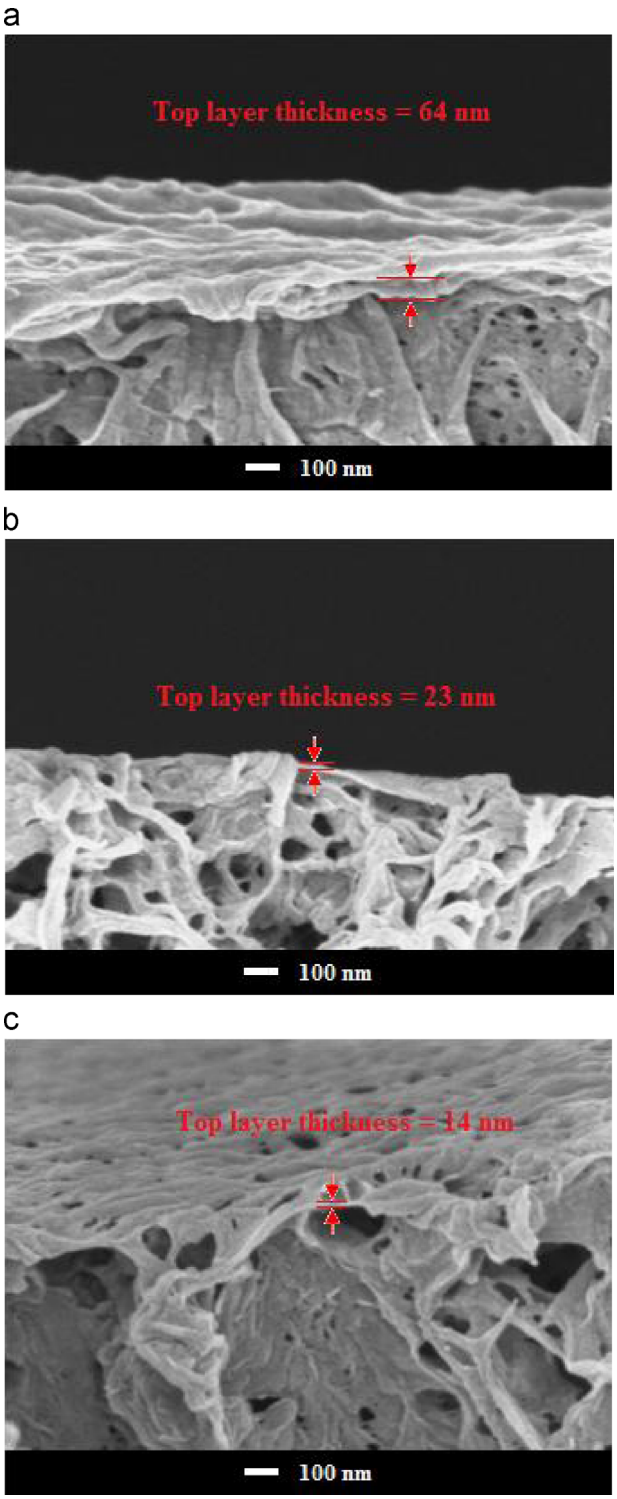

Fig. 3. SEM micrographs of the top skin layer of PVDF membranes: (a) MA; (b) MC; and (c) ME.

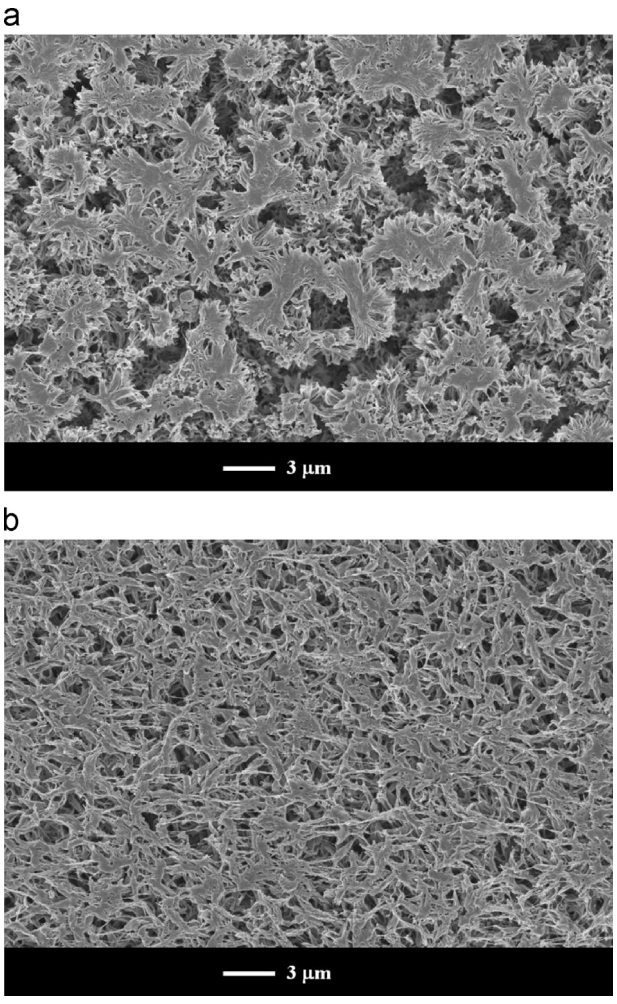

Fig. 4. SEM micrographs of the bottom surfaces of PVDF membranes: (a) MA and (b) ME.

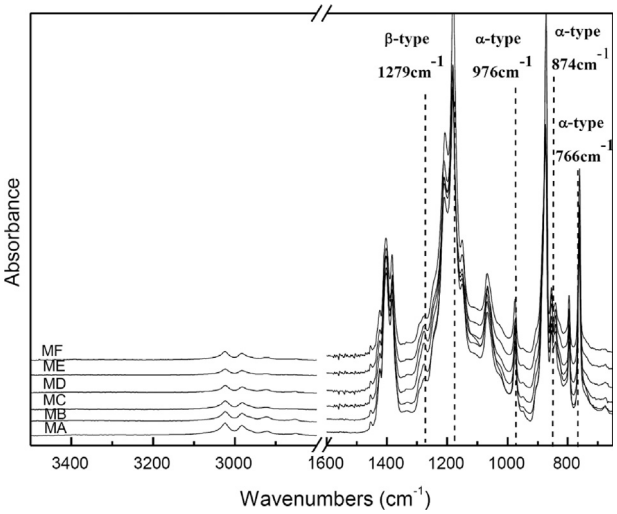

Fig. 5. FTIR spectra of the PVDF membranes.

the membrane. The small doublets at 3024 and 2978 cm^{-1} stand for the symmetric and asymmetric stretching of CH_2 groups in the polymer chains respectively [23,24]. There is no indication of absorption around 3100–3500 cm^{-1} (the hydroxyl groups), implying that Tween-20 is nearly completely removed during the washing steps; even if it does exist in the membrane, the quantity must be lower than the level detectable by FTIR. The above spectroscopic data are different from what Loh et al. has observed for the polyethylsofone membranes prepared using Pluronic (block copolymer of ethylene oxide and propylene oxide) as the pore former, in which case absorptions due to hydroxyl groups can be located in the FTIR spectra [10].

Using NMR analysis, it is possible to determine with reliable accuracy the quantity of residual Tween-20 in the membranes. As an example, Fig. 6 shows the spectrum of the membrane "ME".

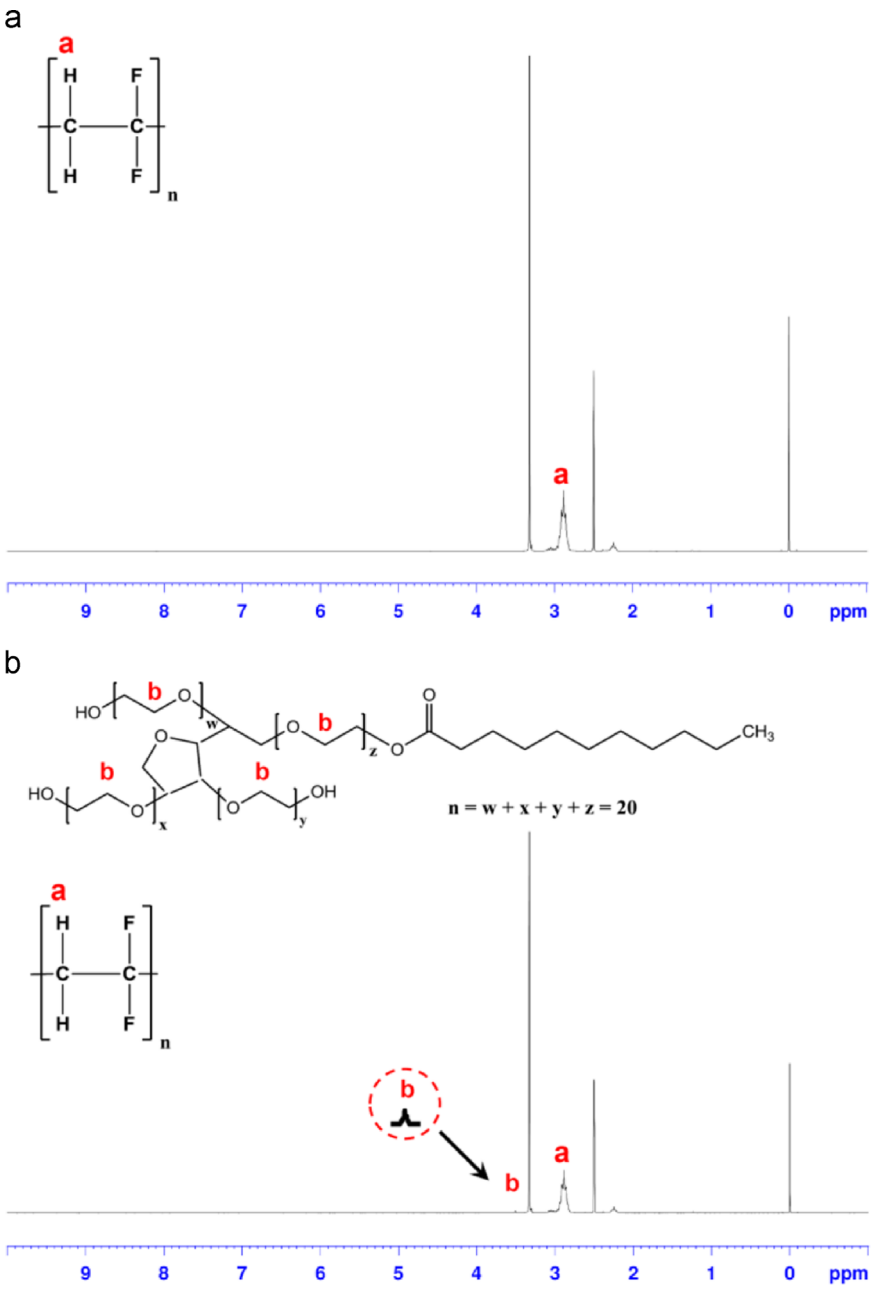

Fig. 6. ^{1}H NMR spectra of the PVDF membranes: (a) MA and (b) ME.

The chemical shifts at zero and 3.3 ppm are due to the NMR-standard TMS and the d-solvent (DMSO-d_6), respectively. The small peaks appearing at 2.9 and 3.5 ppm correspond to the methylene groups of PVDF [19] and ethylene oxide groups of Tween-20 [25], respectively. Based upon Eq. (1), the Tween-20 contents (wt%) in various membranes were determined and the results are listed in Table 3. In consistent with the FTIR analyses, Tween-20 exists only in minuscule amounts. The percentage of remaining Tween-20 increases from 0.08% for the membrane "MB" to 0.54% for the membrane "MF", which amounts to a high extraction efficiency of ~99% for all cases. It has been found in the current investigation that without going through a careful and repeated washing procedure, the residual amount can reach as high as 7.2% (or extraction efficiency of 67%).

In addition to the NMR quantification technique, XPS was also utilized to determine the amount of Tween-20 in the vicinity of the top surface of the membrane. Some typical spectra are presented in Fig. 7 and the calculated percentages based on Eq. (2) are given in Table 3. The atomic ratio of C:F, as shown in the fine scans of the figure, approaches 1:1, agreeing with the chemical structure of PVDF. The slightly higher carbon percentage explains partly the presence of Tween-20 residues on the membrane surface. From

Table 3
The extraction efficiency and residual percentage of Tween-20 in the membranes.

Code	Remaining (NMR) (%)	Extraction efficiency (NMR) (%)	Remaining (XPS) (%)
MA	–	–	–
MB	0.08	98.6	–
MC	0.31	98.1	–
MD	0.35	98.7	3.16
ME	0.47	98.9	–
MF	0.54	99.0	3.71

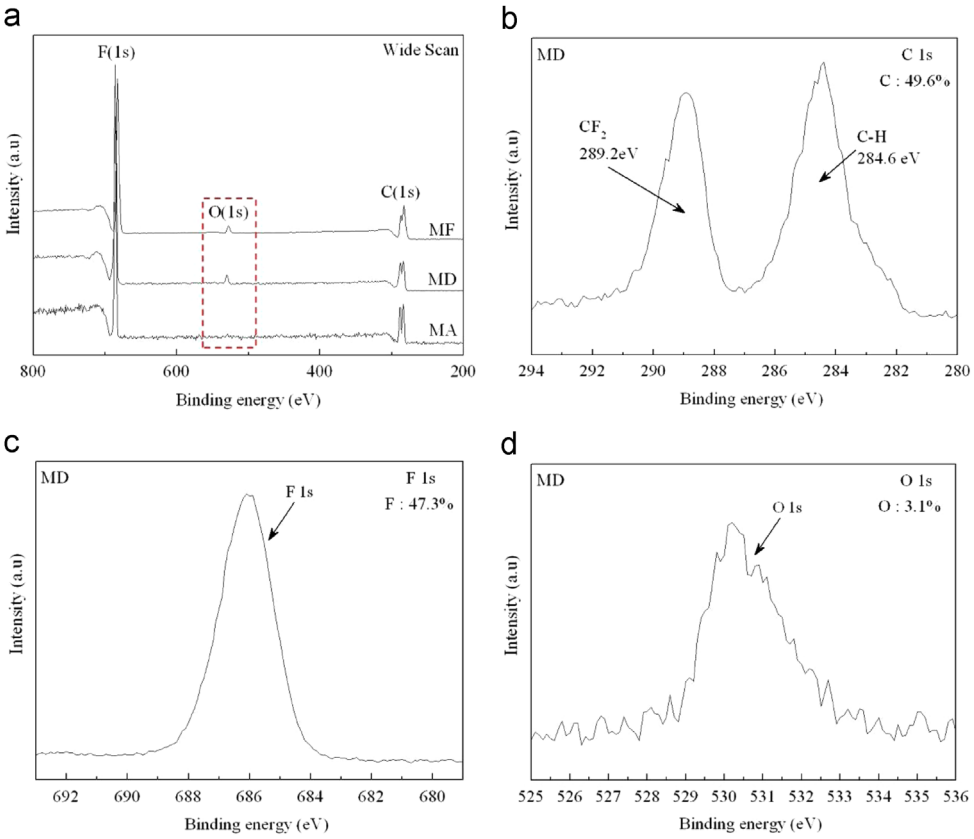

Fig. 7. XPS scanning of the PVDF membranes. (a) The survey scans of MA, MD and MF. (b) The narrow scan of carbon composition of MD. (c) The narrow scan of fluorine composition of MD. (d) The narrow scan of oxygen composition of MD.

Table 3, the Tween-20 contents on the top surfaces of the membranes MD and MF are 3.16% and 3.71%, respectively, largely consistent with the data determined from NMR analyses. They are somewhat higher, implying that some traces of Tween-20 were trapped in the top skin region where the compact structure made it harder for Tween-20 to move across.

Based on the aforementioned morphological characteristics and analytical data, a preliminary mechanism for pore formation is proposed herein. The precipitation process is shown schematically in Fig. 8. Without using Tween-20, it is appropriate to describe the precipitation process as being dominated by crystallization of PVDF (note that the dope is in a meta-stable state with respect to crystallization) [3], which commences with the nucleation of crystalline domains, Fig. 8(a). These nuclei grow by rejection of liquids (largely water and TEP) into the bulk solution resulting in the formation of polymer-rich and polymer-poor phases, Fig. 8(b). The growth process continues until a gelation stage is reached, at which the sheaf-like crystallites impinge each other, and interlocked into a continuous polymeric matrix intertwining with micro-channels of liquid phases, Fig. 8(c). Meanwhile, polymer concentration near the top surface rises rapidly as a result of contacting the harsh nonsolvent; thereby, a robust gel layer is constructed, which decelerates the exchange of solvent and nonsolvent, and eventually becomes a dense top skin. For precipitation with the involvement of Tween-20, it is necessary to account for the escaping behavior of this molecule. Since Tween-20 dissolves readily in water, it would leave the casting solution along with the out-diffusing TEP at the instant of immersion, Fig. 8(d). This activity interrupts the formation of a continuous polymer-rich top layer; therefore, water molecules can enter the casting film to induce liquid–liquid demixing. The formed liquid microdroplets subsequently develop into columnar voids underneath the skin, Fig. 8(e). On the other hand, growth of PVDF nuclei occurs in the bulk of the casting solution, by which a bi-continuous matrix composed of interlocked stick- or sheaf-like spherulites is formed. Because the top gel layer is broken-up by the out-diffusing Tween-20, the formed membrane has a top selective layer containing many nano-pores, Fig. 8(f).

3.3. Physical properties and filtration performance

Bulk porosities of the formed membranes are listed in Table 1. They tend to increase with increasing Tween-20 content in the dope. For the membrane MA, the porosity is only 68%, yet after addition of 10% Tween-20 in the dope, a high porosity of 81% is attained. It is also noted that the porosities of the membranes MD, ME, and MF are close to each other; namely, the pore-forming capability reaches maximum value at ~5% of Tween-20 addition. Further increase of Tween-20 exerts its effects mainly on the top selective layer (Table 2), which is similar to those reported in the literature that used surfactant to enhance pore formation [10,11,13,16]. The tensile strengths of the prepared membranes were measured by a universal testing machine, and the results are summarized in Table 1. Membrane "MA" is quite strong with a tensile strength of 6.9 N/mm^2. A significant drop of the strength to 3.6 N/mm^2 is observed for the membrane "MB", which is largely due to the increased porosity and the presence of columnar voids beneath the top surface of the membrane. Further increase of Tween-20 dosage results in smaller decreases of the tensile strength, and in particular, the tensile strengths of MD, ME, and MF are similar, ~2.2–2.3 N/mm^2 just like the case of porosity. The slight strength difference between these membranes may be associated with the minor nano-scaled differences in size, porosity, and thickness of the skin layer. Water contact angles of the

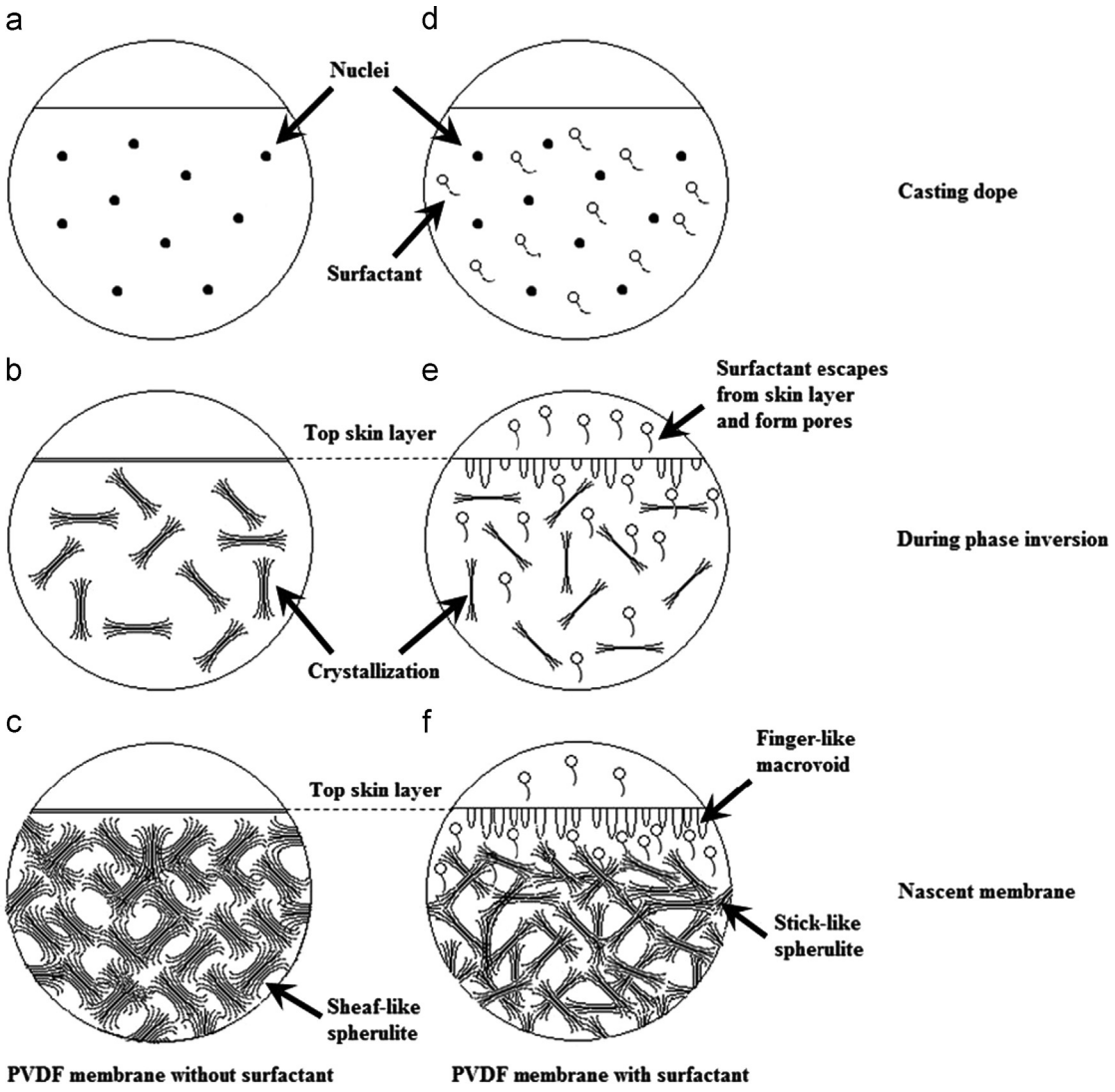

Fig. 8. Schematic representation of the formation mechanism of PVDF membranes with and without the addition of surfactant in the dope.

membranes, as shown in Table 2, fall over the range of 82–86° for the top surfaces, and 108–120° for the bottom surfaces. These values are typical of hydrophobic porous membranes prepared from the immersion–precipitation method. For each membrane, the bottom surface has a higher contact angle than the top surface because the former is very porous while the latter is relatively dense (with very low porosity) [3,26]. The fact that contact angles for various membranes are similar confirms that Tween-20 resides in the vicinity of the surface only in trace amount; for otherwise a significant decrease would be observed (e.g., the contact angle of the top surface becomes 72°, if the membrane contains 7.2% Tween-20 residues) [12,13,15].

Pure water fluxes of various PVDF membranes over the range suited to micro- and ultra-filtrations are shown in Fig. 9. The flux of the membrane "MA" is immeasurably small obviously due to the presence of a dense skin on the membrane's top surface, which effectively prohibits the permeation of water molecules even up to a trans-membrane pressure of 4 kg/cm^2. With increasing Tween-20 dosages, the fluxes increase, agreeing with the top surface morphologies of the membranes, which are particularly important for the membranes MD, ME, and MF. As is evident from Tables 1 and 2, the bulk porosities and thicknesses for these three membranes are close, yet the surface porosity increases from 5.5% (MD) to 15% (MF). Specifically, the pure water flux of the membrane "ME" is

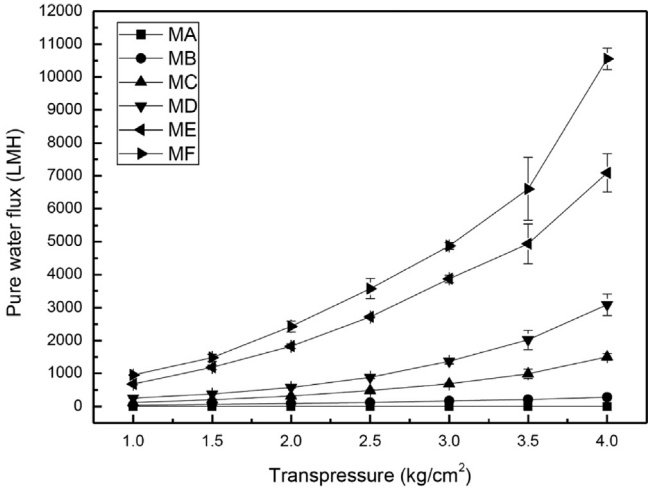

Fig. 9. Pure water fluxes of PVDF membranes.

~680 LMH at 1 kg/cm^2, which is larger than that of the membrane prepared without using pore former but with a *soft* bath containing 50% TEP [3]. For the latter case, the fabrication cost and the environmental impact are considerably higher. Table 4 lists water

Table 4
The water flux at 1 bar of various PVDF membranes from literature.

Membrane material	Additive/bath	Pure water flux (LMH)	Reference
PVDF	7.5% Tween-20/H_2O	680	This study
PVDF	N.A./50% TEP solution	300	[3]
PVDF	2% EPTBP/H_2O	750	[15]
PVDF	2% HPE-g-MPEG/H_2O	525	[15]
PVDF	2% ACPS/H_2O	420	[15]
PVDF	2% PEG/H_2O	500	[15]
PVDF/PES	5% PVP/H_2O	330	[27]

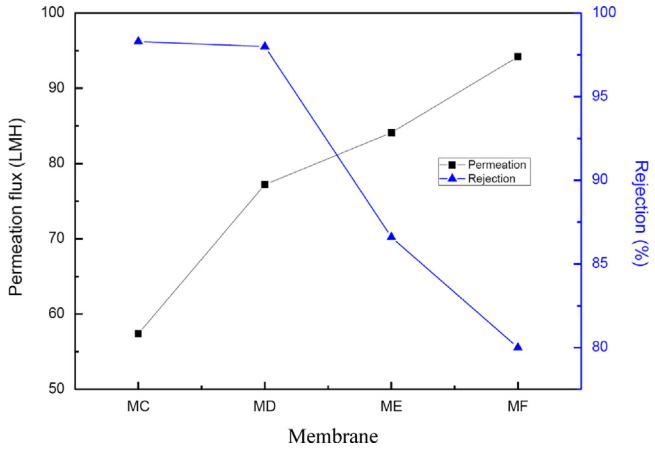

Fig. 10. The rejection coefficients and the permeation fluxes of PVDF membranes. (*Note*: for "MA" and "MB", flux ≈ 0 LMH.)

flux data for PVDF membranes prepared with employment of various kinds of pore formers documented in the literature. The values are on the same order as the present membrane "ME" [15,27], validating the measured flux data being reliable. Filtration performances (0.1% blue dextran solution) of various membranes have been examined [22,28–31], and the results are presented in Fig. 10. As is expected, the filtrate fluxes increase but the rejection coefficients decrease from the membranes "MC" to "MF". For "MC" and "MD", the rejection coefficient reaches as high as ~97%, while it becomes only ~80% for the membrane "MF". Conversely, the filtrate flux of the membrane "MF" is ~1.7 times that of "MC". Zhang et al. reported a dextran (70 kDa) rejection of ~84–87% for PVDF membranes prepared using Tween-80/water mixtures as additives [28]. By changing the spinning parameters, Abed et al. were able to prepare ultrafiltration hollow fiber membranes with different MWCO (40–200 kDa) [29]. Loh and Wang used dual additives, Pluronic plus LiCl, to form high performance hollow fibers having high water flux of 2530 $Lm^{-2}\,h^{-1}\,MPa^{-1}$ and low MWCO of 53 kDa [22]. Generally, these membranes have lower MWCO than the present membranes "MC–MF", which is considered to be due to their smaller pore sizes. In summary, it may be stated that by adding a small amount of additives in the casting dope, it is possible to prepare membranes with appropriate porous structures that allow ultra-filtration operations.

4. Conclusions

Using Tween-20 as a pore former, formation of porous PVDF membranes via the isothermal immersion–precipitation process was investigated. The formed membranes exhibit an uncommon type of morphology being composed of a thin nano-porous top layer, followed by a short region of columnar voids, and then a thick bi-continuous porous support. By adjusting the Tween-20 content in the dope, it is possible to vary the size and quantity of pores on the top surface, and the porosity in the bulk of the membrane. For example, the average size of pores on the top surface increases from 26 to 43 nm, and pore fraction from 1.9% to 15%, when the added Tween-20 is raised from 1% to 10%. The amounts of Tween-20 remained in the formed membranes were determined both by ^{1}H NMR and XPS spectroscopic analyses. It is found that almost all Tween-20 has been removed during the precipitation and/or washing steps, with a low residue fraction of ~1% of the initially loaded Tween-20. The separation performances of the prepared PVDF membranes were tested via ultrafiltration of blue dextran (2000 kDa) solutions. The results indicate that the filtrate flux increases while rejection coefficient decreases for membranes prepared from dopes with increasing Tween-20 content, which is consistent with the morphological features of the tested membranes.

Acknowledgment

The authors would like to thank the Ministry of Science and Technology in Taiwan (NSC 99-2221-E-032-002-MY3) for the financial support.

Appendix A. Supporting information

Supplementary data associated with this article can be found in the online version at http://dx.doi.org/10.1016/j.memsci.2014.05.011.

References

[1] F. Liu, N.A. Hashim, Y. Liu, M.R.M. Abed, K. Li, Review – progress in the production and modification of PVDF membranes, J. Membr. Sci. 375 (2011) 1–27.
[2] H.H. Chang, S.C. Chen, D.J. Lin, L.P. Cheng, Preparation of bi-continuous Nylon-66 porous membranes by coagulation of incipient dopes in soft non-solvent baths, Desalination 313 (2013) 77–86.
[3] D.J. Lin, H.H. Chang, T.C. Chen, Y.C. Lee, L.P. Cheng, Formation of porous poly (vinylidene fluoride) membranes with symmetric or asymmetric morphology by immersion precipitation in the Water/TEP/PVDF system, Eur. Polym. J. 42 (2006) 1581–1594.
[4] A.J. Reuvers, C.A. Smolders, Formation of membranes by means of immersion precipitation. Part II. The mechanism of formation of membranes prepared from the system CA/acetone/Water, J. Membr. Sci. 34 (1987) 67–86.
[5] L.P. Cheng, Effect of temperature on the formation of microporous PVDF membranes by precipitation from 1-Octanol/DMF/PVDF and Water/DMF/PVDF systems, Macromolecules 32 (1999) 6668–6674.
[6] D.J. Lin, C.L. Chang, F.M. Huang, L.P. Cheng, Effect of salt additive on the formation of microporous poly(vinylidene fluoride) membranes by phase inversion from $LiClO_4$/Water/DMF/PVDF system, Polymer 44 (2003) 413–422.
[7] E. Drioli, A. Ali, S. Simone, F. Macedonio, S.A. Al-Jlil, F.S. Al Shabonah, H.S. Al-Romaih, O. Al-Harbi, A. Figoli, A. Criscuoli, Novel PVDF hollow fiber membranes for vacuum and direct contact membrane distillation applications, Sep. Purif. Technol. 115 (2013) 27–38.
[8] M.R. Mogharen Abed, S.C. Kumbharkar, A.M. Groth, K. Li, Ultrafiltration PVDF hollow fiber membranes with interconnected bicontinuous structures produced via a single-step phase separation technique, J. Membr. Sci. 407–408 (2012) 145–154.
[9] T.M. Don, Y.C. Hsu, H.Y. Tai, E. Fu, L.P. Cheng, Preparation of bi-continuous macroporous polyamide copolymer membranes for cell culture, J. Membr. Sci. 415–416 (2012) 784–792.
[10] C.H. Loh, R. Wang, L. Shi, A.G. Fane, Fabrication of high performance polyethersulfone UF hollow fiber membranes using amphiphilic Pluronic block copolymers as pore-forming additives, J. Membr. Sci. 380 (2011) 114–123.
[11] A. Rahimpour, S.S. Madaeni, Y. Mansourpanah, The effect of anionic, non-ionic and cationic surfactants on morphology and performance of polyethersulfone ultrafiltration membranes for milk concentration, J. Membr. Sci. 296 (2007) 110–121.
[12] N. Ghaemi, S.S. Madaeni, A. Alizadeh, P. Daraei, V. Vatanpour, M. Falsafi, Fabrication of cellulose acetate/sodium dodecyl sulfate nanofiltration membrane: characterization and performance in rejection of pesticides, Desalination 290 (2012) 99–106.
[13] N. Ghaemi, S.S. Madaeni, A. Alizadeh, P. Daraei, A.A. Zinatizadeh, F. Rahimpour, Separation of nitrophenols using cellulose acetate nanofiltration membrane: Influence of surfactant additives, Sep. Purif. Technol. 85 (2012) 147–156.

[14] H.A. Tsai, L.D. Li, K.R. Lee, Y.C. Wang, C.L. Li, J. Huangc, J.Y. Lai, Effect of surfactant addition on the morphology and pervaporation performance of asymmetric polysulfone membranes, J. Membr. Sci. 176 (2000) 97–103.
[15] Y.H. Zhao, Y.L. Qian, B.K. Zhu, Y.Y. Xu, Modification of porous poly(vinylidene fluoride) membrane using amphiphilic polymers with different structures in phase inversion process, J. Membr. Sci. 310 (2008) 567–576.
[16] M. Amirilargani, E. Saljoughi, T. Mohammadi, Effects of Tween-80 concentration as a surfactant additive on morphology and permeability of flat sheet polyethersulfone (PES) membranes, Desalination 249 (2009) 837–842.
[17] N. Riyasudheen, A. Sujith, Formation behavior and performance studies of poly (ethylene-co-vinyl alcohol)/poly(vinyl pyrolidone) blend membranes prepared by non-solvent induced phase inversion method, Desalination 294 (2012) 17–24.
[18] D.M. Wang, F.C. Lin, T.T. Wu, J.Y. Lai, Formation mechanism of the macrovoids induced by surfactant additives, J. Membr. Sci. 142 (1998) 191–204.
[19] Y.W. Kim, D.K. Lee, K.J. Lee, J.H. Kim, Single-step synthesis of proton conducting poly(vinylidene fluoride) (PVDF) graft copolymer electrolytes, Eur. Polym. J. 44 (2008) 932–939.
[20] D.J. Lin, K. Beltsios, T.H. Young, Y.S. Jeng, L.P. Cheng, Strong effect of precursor preparation on the morphology of semicrystalline phase inversion poly (vinylidene fluoride) membranes, J. Membr. Sci. 274 (2006) 64–72.
[21] S.A. McKelvey, W.L. Koros, Phase separation, vitrification, and the manifestation of macrovoids in polymeric asymmetric membranes, J. Membr. Sci. 112 (1996) 29–39.
[22] C.H. Loh, R. Wang, Effects of additives and coagulant temperature on fabrication of high performance PVDF/Pluronic F127 blend hollow fiber membranes via nonsolvent induced phase separation, Chin. J. Chem. Eng. 20 (2012) 71–79.
[23] S.L. Méndez, J.F. Mano, A.M. Costa, V.H. Schmidt, FTIR and DSC studies of mechanically deformed PVDF films, J. Macromol. Sci. Part B Phys. 40 (2001) 517–527.
[24] S.H. Choi, F. Tasselli, J.C. Jansen, G. Barbieri, E. Drioli, Effect of the preparation conditions on the formation of asymmetric poly(vinylidene fluoride) hollow fibre membranes with a dense skin, Eur. Polym. J. 46 (2010) 1713–1725.
[25] M. Verbrugghe, P. Sabatino, E. Cocquyt, P. Saveyn, D. Sinnaeve, P.V. Meeren, J. C. Martins, Solubilization of flurbiprofen with non-ionic Tween-20 surfactant micelles: a diffusion ^{1}H NMR study, Colloids Surf. A Physicochem. Eng. Asp. 372 (2010) 28–34.
[26] H.H. Chang, K. Beltsios, D.J. Lin, L.P. Cheng, Formation of polyamide 12 membranes via thermal-nonsolvent induced phase separation, J. Appl. Polym. Sci. 130 (2013) 14–24.
[27] L. Wu, J. Sun, Q. Wang, Poly(vinylidene fluoride)/polyethersulfone blend membranes: effects of solvent sort, polyethersulfone and polyvinylpyrrolidone concentration on their properties and morphology, J. Membr. Sci. 285 (2006) 290–298.
[28] P.Y. Zhang, H. Yang, Z.L. Xu, Preparation of polyvinylidene fluoride (PVDF) membranes via nonsolvent induced phase separation process using tween 80 and H_2O mixture as an additive, Ind. Eng. Chem. Res. 51 (2012) 4388–4396.
[29] M.R. Moghareh Abed, S.C. Kumbharkar, A.M. Groth, K. Li, Ultrafiltration PVDF hollow fiber membranes with interconnected bicontinuous structures produced via a single-step phase inversion technique, J. Membr. Sci. 407–408 (2012) 145–154.
[30] S.H. Zhi, J. Xu, R. Deng, L.S. Wan, Z.K. Xu, Poly(vinylidene fluoride) ultrafiltration membranes containing hybrid silica nanoparticles: preparation, characterization and performance, Polymer 55 (2014) 1333–1340.
[31] P.C.Y. Wong, Y.N. Kwon, C.S. Criddle, Use of atomic force microscopy and fractal geometry to characterize the roughness of nano-, micro-, and ultrafiltration membranes, J. Membr. Sci. 340 (2009) 117–132.